Tạp chí Khoa học và Công nghệ **54** *(3) (2016) 366-376*

DOI: 10.15625/0866-708X/54/3/7186

EFFECT OF LASER POWER ON THE MOLTEN POOL TEMPERATURE AND LAYER THICKNESS AT THE CURVATURE RADIUS OF THIN-WALL PART FABRICATED BY LASER DIRECT METAL FORMING

Doan Tat Khoa

Military Technical Academy, 236 Hoang Quoc Viet str., Nam Tu Liem Dist., Hanoi, Vietnam

Email: *doankhoactm@gmail.com*

Received: 25 September 2015; Accepted for publication: 30 December 2015

ABSTRACT

To discuss the effect of laser power on the molten pool temperature and layer thickness at the curvature radius of thin-wall parts, the numerical simulation and experimental was studied. The numerical results showed that the molten pool temperature of the thin-wall increases with the layer number, and the molten pool temperature of thin-wall cylinders were increased when curvature radius decreased. The rules of laser power changing with the layer number and curvature in the processing of the thin-wall blade can be obtained when keeping molten pool temperature stable. According to the numerical results, the thin-wall blades were fabricated by experiments. The experimental results showed that the excessive build-up occurred and unevenness thickness layer at small radius corner with constant laser power because of the increase of energy density at corners, while varied laser power is more uniform than the constant laser power, which is in agreement with the numerical simulation.

Keywords: laser direct metal forming, temperature field, curvature, thin-wall part.

1. INTRODUCTION

Laser direct metal forming (LDMF) is a novel layer additive manufacturing technology. There are some other similar technologies using the same principle as LDMF such as Laser Engineered Net Shaping (LENS), Direct Metal Deposition (DMD) etc, which base on rapid prototyping and laser cladding technique. It has been a hot topic in the advanced manufacturing fields, in which, dense metal parts can be fabricated directly from CAD files line by line and layer by layer without constraints on part shape and powder material and without using any tooling. The LDMF supports many types of metals including stainless steels (316 and 304); Ni based super-alloys (Inconel 625, 690, and 718, FGH95, DZ408, DZ125L); cobalt-chrome, and Ti-6Al-4V titanium alloy [1 - 5].

Control of the molten pool size, which is dependent on the molten pool temperature, is a critical issue since it impacts the quality of the product. Therefore, a thorough understanding of the molten pool temperature distribution is imperative. Much research work has been carried out in this field. Pinkerton and Li developed a simple thermal model to analyze the temperature distribution and estimate the molten pool size [6]. Liu and Li established a model to investigate the effects of process parameters on the layer thickness, powder utilization rate, and forming speed of thin-wall parts [7] Labudovic et al studied the effects of laser-processing parameters (laser power and scanning speed) on the molten pool size [8]. Wang et al. developed a three-dimensional finite element model to optimize molten pool size for each layer [9, 10].

In this paper, the effect of temperature field distribution on the curvature change and unevenness thickness layer of thin-wall turbine blade part with different curvature as shown in Fig.1 was studied by simulation and experimental.

Ni-based super-alloys, e.g., Inconel 625, 718 and Rene41, 88DT, DZ125L due to an improved balance of creep, damage tolerance, tensile properties, and corrosion oxidation resistance, are normally developed for high-performance components in jet engines and gas turbines. The super-alloy DZ125L was to be used for this researched.

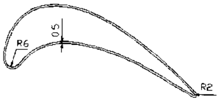

Figure 1 Thin-wall turbine blade mode. (a) three-dimension model, (b) cross section of dimension.

2. THE NUMERICAL SIMULATION TEMPERATURE FIELD

The effect of the temperature field distribution on the curvature change and number layer was simulation by thin-wall cylinders with different curvatures. The thin-wall cylinders with different curvatures can be replaced by different radiuses.

2.1. Analysis model of thin-wall cylinders design

2.1.1. Geometric model

A three-dimensional finite element model of cylinders was built to simulate the LDMF process using ANSYS software. The geometry and finite element mesh used in the model are shown in Fig. 2. The thin-wall cylinder dimensions is: radius 10 mm, height 1.5 mm, thickness 0.5 mm, substrate dimensions is 40×30×8 mm^3

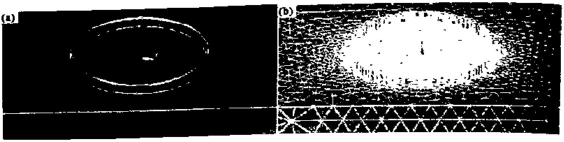

Figure 2. The thin-wall cylinder model: (a) geometric model; (b) element model.

2.1.2. Element birth and death technique

"Element birth and death" technique is usually used to simulate welding and cutting. It does not actually remove "killed" elements from model. Instead, it deactivates them by multiplying their stiffness or conductivity by a severe reduction factor. This factor is set to 1.0×10^{-6} by default, and it can be set to other values. Element loads associated with deactivated elements are zero out of the load vector, but they still appear in element-load lists. The mass, damping and specific heat of deactivated elements was all set to zero likewise.

Similarly, when elements are "born", they are not actually added to the model but simply reactivated. So, we must create all elements in preprocessor, including those to be born in later stages of the analysis. When an element is reactivated, its stiffness, mass and element loads, etc., return to their full original values, but there is no record of strain history for it.

2.1.3. Material properties

The thermal physical behaviors of nickel based supper-alloy DZ125L as shown in Table 1 [11].

2.1.4. The heat transfer model

The heat flux to system is put in by a highly focused area on the molten pool and it is assumed that the heat flux, *q(r)*, follows Gauss distribution in the radial direction, and has the following form [12]:

$$q(r)=\frac{3Q}{\pi R^2}\exp\left(-\frac{3r^2}{R^2}\right) \tag{1}$$

where: R is the laser spot radius (mm); Q is the total input laser energy (W).

5) Boundary conditions

To resolve heat transfer equations, the initial and boundary conditions are needed in the computational domain. The three boundary conditions can be concluded as follows:

$$T=T^{*} \tag{2}$$

$$K_x\frac{\partial T}{\partial x}n_x+K_y\frac{\partial T}{\partial y}n_y+K_z\frac{\partial T}{\partial z}n_z=q \tag{3}$$

$$K_x \frac{\partial T}{\partial x} n_x + K_y \frac{\partial T}{\partial y} n_y + K_z \frac{\partial T}{\partial z} n_z = h(T_a - T) \quad (4)$$

where: K is the thermal conductivity (W/m.°C); h is the convective heat transfer coefficient ($W/m^2.°C$); T_a is the ambient temperature around the part, which is considered to be equal to room temperature (°C)

Besides all the heat conduction equations boundary conditions, the initial temperature must be set, which is considered as initial condition.

$$T(x, y, z)\big|_{t=0} = T_0 \quad (5)$$

The latent heat of fusion is simulated by a manual input in the specific heat according to Labudovic [13]. The relationship among enthalpy (H), density (ρ), and specific heat (c) is

$$\Delta H(T) = \int_0^T \rho c(t)dt \quad (6)$$

where: H is the enthalpy (J/kg).

Table1 Thermal physical behaviors of nickel based supper-alloy DZ125L.

Temperature (°C)	Coefficient thermal of expansion (1/°C)	Density (kg/m^3)	Thermal conductivity (W/m °C)	Thermal capacity (J/kg.°C)	Poison's ratio
20	1.48×10^{-5}	8230	8.0	350	0.33
200	1.52×10^{-5}	8230	9.67	385	0.33
400	1.56×10^{-5}	8230	13.44	456	0.33
600	1.62×10^{-5}	8230	16.79	498	0.33
800	1.69×10^{-5}	8230	19.63	506	0.34
1000	1.75×10^{-5}	8230	19.43	473	0.35
1100	1.80×10^{-5}	8230	19.00	443	0.35

2.2. Simulation results

The numerical results showed that the molten pool temperature of the thin-wall increases with the layer number when keeping laser power, as shown in Fig. 3(a). In order to achieve a steady temperature distribution surrounding the molten pool, the laser power must be adjusted for each layer. Provided that the laser power of the first deposition layer is denoted by P, the declined percentages of laser power are denoted by α with the increasing layer number when the temperature of each layer is consistent with the temperature of the first layer. Then the laser power of any layer can be calculated by P×α ($0.8 \le \alpha \le 1$) under keeping the molten pool temperature of each layer stable, as shown in Fig. 3(b). It is observed that the laser power decreases with the layer number [14].

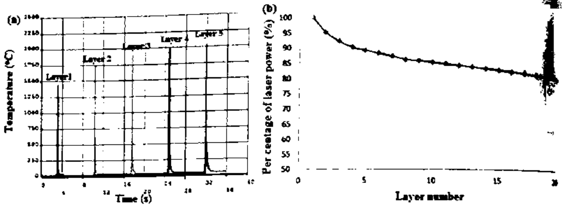

Figure 3. The relationship between molten pool and layer number.

The thin-wall cylinders with different curvatures can be handled by defining different radiuses. To investigate the influence of different thin-wall cylinder's radiuses on the molten pool temperature, the molten pool temperature distribution is studied with the radius of R = 2, 4, 6, 8, 10, and 20 mm. Fig.4 showed the typical temperature field distributions of the thin-wall cylinders with the radius of 2 and 6 mm. The relationship between temperature distribution and radius is shown in Fig. 5.

The Fig. 5 shows that, the molten pool temperature decreases with the radius, namely, the molten pool temperature increases with the curvature. It is also observed that the molten pool temperature tends to be gentle when the radius is more than 6 mm. This indicates that the influence of the radius on the molten pool temperature is weak when the radius is more than 6 mm.

In order to keep the molten pool temperature stable for different radiuses, the trend of laser power changing can be obtained based on the 1650 °C produced by temperature field computation of the thin wall's first layer. And the relationship between laser power and radius was shown in Fig. 6.

The laser power of any layer can be calculated by P = P(x) under keeping the molten pool temperature of each layer stable. To keep the temperature distributions of the thin-wall cylinders with different curvatures consistent with the thin wall, the decline percentages of laser power are denoted by P = P(y) with the increasing curvature. So, the trend of laser power changing with layer number and curvature can be obtained under keeping melt pool temperature stable. The laser power of the first deposition layer used is denoted by P_0. The relationship between laser power with layer numbers and curvature:

$$P_{xy} = P_0 e^{\alpha x+\beta y+\gamma} \tag{7}$$

where, x is the layer numbers; y is the curve radius; α, β,γ are **coefficient**.

Using linear regression least square method, the discrete points in Fig 3(b) and Fig 6 can get equation:

$$P_{xy} = P_0 e^{-0.016x+0.055y-0.016} \tag{8}$$

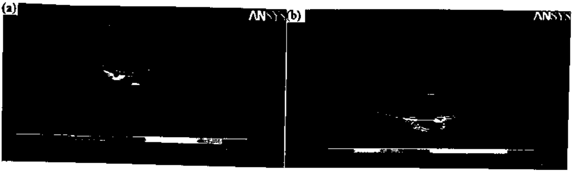

Figure 4 The temperature field distribution with different radius; (a) R = 2 mm; (b) R = 6 mm

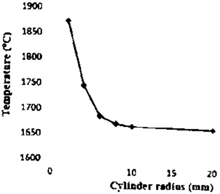

Figure 5 The relationship between temperature distribution and radius

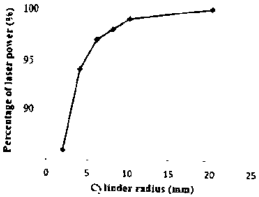

Figure 6 The trend of laser power changing with different radius

3. EXPERIMELTAL PROCEDURES

3.1. Materials and equipment

The experiments were carried out by the system as shown in Fig 7 The LDMF process includes a Nd:YAG laser with a 1 kW maximum output power (wavelength 1063 nm, spot diameter of 0.5 mm, the laser beam was guided to the workstation through an optical fiber and focused by an optic) and a three-axis CNC linkage worktable and a powder feeder with a coaxial feeding nozzle and a gas protection device. The processing chamber of the system was protected from oxidation by argon gas

The powder used was nickel based super-alloy DZ125L with spherical shape and smooth surface Additionally, the DZ125L particle size distributes of about 30–60 μm and the mean particle size of about 45 μm The substrate was the same material, and its dimension was 150×100×8 mm. The compositions of the powder and the substrate are shown in Table 2

3.2. Processing

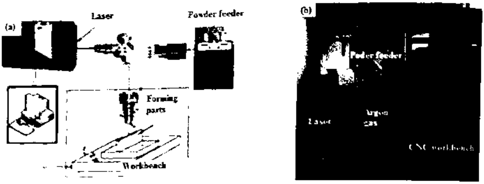

Figure 7. The LDMF system (a) schematic diagram of experiment, (b) the real workshop of experiment setup.

To agree with simulation computation, the process parameters are shown in Table 3. The thin-wall blade samples were built with two different conditions: constant laser power and varied laser power. The layer number of the two parts is 30. According to numerical results, the varied laser power was carried out as follows: the laser power is changed with layer number, and in each layer the laser power is also different at the corners of R = 2 mm and R – 6 mm in Fig. 1 and the varied laser power as shown in Table 4. The pictures of the two parts with 30 layers are shown in Fig. 8 and Fig. 9. After experiments the cross sections of thin-walled blade samples were obtained by cutting, grinding, polishing and metallographical etching, and then the thickness of each layer can be measured under Optical Microscope (VH-8000, made in Japan by the KEYENCE).

Table 2. Material compositions of the substrate and the powder (%).

Material	C	Cr	Co	Mo	W	Al	Ti	Ta	B	Ni
Substrate	0.07	9.09	10.00	2.09	7.17	4.48	3.05	3.64	0.011	Balance
Powder	0.09	9.70	9.64	2.18	7.14	4.90	3.12	3.78	0.015	Balance

Table 3. Process parameters for fabrication of thin-wall cylinder parts.

Laser power (W)	Powder mass flow rate (g/min)	Table feeding rate (mm/s)	Beam diameter (mm)	Z-increment (mm)	Deposition distance (mm)
230-160	6.5	10	0.5	0.07	5

Table 4. The varied laser power on the thin-wall turbine blade fabricated by LDMF

Layer numbers	Coefficient α	Coefficient β	Laser power P_{ij} (W)
		$R \geq 6$ $\beta \sim 1$	230
		$R - 2 \cdot \beta = 0.86$	198
2-5	0.9	$R \geq 6 \cdot \beta = 1$	207
		$R = 2 \cdot \beta = 0.86$	178
6-8	0.87	$R \geq 6 \cdot \beta = 1$	200
		$R = 2 \cdot \beta = 0.86$	172
9-12	0.85	$R \geq 6$: $\beta = 1$	195
		$R = 2.$ $\beta = 0.86$	168

13-15	0.83	$R \geq 6, \beta = 1$ $R = 2, \beta = 0.86$	190 165
16-30	0.8	$R \geq 6, \beta = 1$ $R = 2; \beta = 0.86$	185 160

3.3. Experimental results and discussion

Figure 8 shows the sample fabricated with the constant laser power of 230 W. We can see that the height on the top layer of the sample is uneven, and the corner is abnormally higher than other places in the scanning path. Because, at the sharp corners in the path, the energy and powders higher than other normal places. As a result, the effects resulted in excessive build-up. Simultaneously, the thickness of the thin-wall blade is increased from the bottom to the top as showed that Fig. 8(b, c, d). This is due to the change of the molten pool temperature field distribution during the whole depositing process. As displayed in Fig. 3(a), it can be recognized that at the beginning the temperature increased very rapidly with the layer number because the work-piece was cold and the heat conductivity (three dimensional) was high and the thickness is non-uniform in the first a few layers. After about 15 layers, with decreasing heat conduction (two dimensional), the heat exchange reached a quasi-steady status. Thus, the molten pool temperature increased slowly.

To improve the forming quality of the sample and control, the molten pool temperature, the varied laser power was pre-set in CNC system according to the numerical results. Figure 9 shows the sample and its cross section, its exhibits no excessive build-up but a homogeneous thickness. The thicknesses with layer number were measured at two positions: position 1 (R = 6 mm) and position 2 (R = 2 mm) under the two laser power of different conditions. Fig. 8(d) and Fig. 9(d) showed the relationship between layer thickness and layer number under two laser power conditions, respectively.

As can be seen from Fig. 8(d), the layer thickness increases gradually with the layer number and decreases with the radius. Fig. 9(d) shows that the thickness of the sample is uniform compared to Fig. 8(d) under the varied laser power condition.

By using above parameters, a thin-wall blade sample was fabricated as shown in Fig.10. The actual building height of the thin-wall blade sample is 69.8 mm, and the designed height is 70 mm.

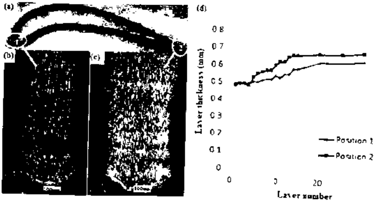

Figure 8. The thin-wall blade samples fabricated by constant laser power. (a) thin-wall blade sample, (b) position 1 of cross sections, (c) position 2 of cross sections, (d) the relationship between layer thickness and layer number.

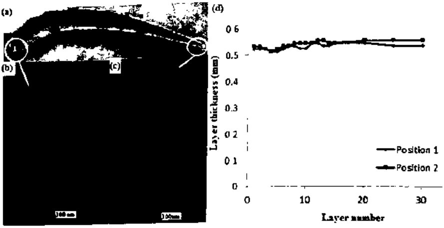

Figure 9. The thin-wall blade samples fabricated by varied laser power. (a) thin-wall blade sample; (b) position 1 of cross sections; (c) position 2 of cross sections; (d) the relationship between layer thickness and layer number.

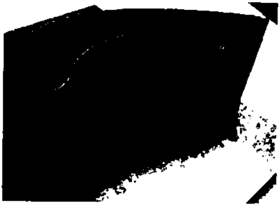

Figure 10. The thin-wall blade fabricated by varied laser power.

4. CONCLUSIONS

The temperature field distribution of thin-wall part by LDMF was studied by numerical simulation. The simulation results showed that the trend of laser power changing with the layer number and curvature in the processing of the thin-wall blade can be obtained when keeping molten pool temperature stable. According to the simulation result, the effect of laser power on the layer thickness and curvature change of thin-wall part were experimentally studied, showing that the excessive build-up occurred with constant laser power because of the increase of energy density at corners, with varied laser power is more uniform than the constant laser power.

REFERENCES

1. Wang H. M, Duan G. - Wear and corrosion behavior of laser clad Cr_3Si reinforced intermetallic composite coatings, Intermetallic **11** (2003) 755-762.

2. Tan H., Chen J. - Process analysis for laser solid forming of thin-wall structure. Int J. Mach. Tools Manu **50** (2010) 1-8.
3. Wohlers Associates - Additive Manufacturing and 3D Printing State of the Industry, Annual Worldwide Progress Report **7** (2011) 384-389.
4. J. Choi, B. Dutta. - Spatial Control of Crystal Texture by Laser DMD Process, Supplemental Proceedings **1** (2009) 405-413
5. Venkatakrishanan K., Sivakumar N. R. - Direct fabrication of surface-relief grating by interferometric technique using femtosecond laser, Appl. Phys. A Mater. Sci. Process. **77** (2003) 959-963
6. Pinkerton A. J, Li. L. - The significance of deposition point standoff variations in multiple-layer coaxial laser cladding coaxial cladding standoff effects, International Journal of Machine Tools & Manufacture **44** (2014) 573-584.
7. Liu J. C, Li. L. - Effects of process variables on laser direct formation of thin wall, Optics and Laser Technology **39** (2007) 231-236.
8. Labudovic. M, Hu. D, Kovacevic. R - A three dimensional model for direct laser metal powder deposition and rapid prototyping, J. Mater. Sci **38** (2003) 35–49
9. Wang. L, Felicelli. S, Gooroochurn Y - Optimization of the LENS process for steady molten pool size, Mater. Sci Eng. **474** (2008) 148–156.
10. Wang. L, Felicelli. S. - Analysis of thermal phenomena in LENS deposition, Mater. Sci. Eng. **435** (2006) 625–631.
11. Zhou C., Wang N , Xu H. - Comparison of thermal cycling behavior of plasma-sprayed nanostructured and traditional thermal barrier coatings, Materials Science and Engineering, A **452–453** (2007) 569-574.
12. Rong L. Sh, Liu. W. J – Numerical simulation of thermal behavior during laser metal shaping, Trans nonferrous Met. Soc. China **18** (2008) 691-699.
13. Labudovic M – A three dimensional model for direct laser metal powder deposition and rapid prototyping, Journal of Material Science **38** (2003) 35-49.
14. DoanTat Khoa - The effect of laser power on the uniform thickness of the thin-wall part fabricated by the laser direct metal forming technology, Journal of Science and Technology **53** (4) (2015) 493-503.

TÓM TẮT

ẢNH HƯỞNG CỦA CÔNG SUẤT LASER ĐẾN NHIỆT ĐỘ VÙNG NÓNG CHẢY VÀ CHIỀU DÀY LỚP TẠO HÌNH TẠI VÙNG CÓ ĐỘ CONG KHÁC NHAU CỦA CHI TIẾT THÀNH MỎNG CHẾ TẠO BỞI CÔNG NGHỆ TẠO HÌNH BẰNG TIA LASER

Đoàn Tất Khoa

Học viện Kỹ thuật quân sự, 236 Hoàng Quốc Việt, Bắc Từ Liêm, Hà Nội

Email: *doankhoactm@gmail.com*

Bài báo sử dụng phương pháp mô phỏng kết hợp với thực nghiệm để nghiên cứu sự ảnh hưởng của công suất nguồn laser đến nhiệt độ vùng nóng chảy và chiều dầy lớp tạo hình tại vùng có độ cong khác nhau của chi tiết thành mỏng. Kết quả mô phỏng cho thấy nhiệt độ vùng nóng chảy tăng lên khi số lớp tạo hình tăng lên và bán kính cong giảm xuống; đã tìm ra quy luật thay đổi công suất nguồn laser so với số lớp tạo hình và theo sự thay đổi bán kính cong để giữ cho nhiệt độ vùng nóng chảy luôn ổn định tại mọi vị trí. Dựa theo kết quả mô phỏng đã thí nghiệm tạo hình chi tiết cánh tua bin thành mỏng. Kết quả thí nghiệm cho thấy khi giữ công suất nguồn laser không đổi trong suốt quá trình tạo hình thì chi tiết thành mỏng xuất hiện vấu lồi và chiều dầy thành mỏng tăng theo số lớp tạo hình tại vùng có bán kính cong nhỏ, đó là do sự tập trung mật độ năng lượng lớn tại các góc có bán kính cong nhỏ; khi thay đổi công suất laser theo quy luật tìm được thì chế tạo được chi tiết cánh tua bin thành mỏng có chất lượng bề mặt tốt và chiều dầy đồng đều ở mọi vị trí, điều này phù hợp với kết quả mô phỏng.

Từ khóa: công nghệ tạo hình bằng tia laser, trường nhiệt độ, độ cong, chi tiết thành mỏng.